Electronic Supplementary Information

Mixed-valence copper(I,II) complexes with 4-(1*H*-pyrazol-1-yl)-6-R-pyrimidines: from ionic structures to coordination polymers

Katerina A. Vinogradova[a,b], Viktor P. Krivopalov[c], Elena B. Nikolaenkova[c], Natalia V. Pervukhina[a], Dmitrii Yu. Naumov[a,b], Evgenii G. Boguslavsky[a] and Mark B. Bushuev [a,b,*]

[a] *Nikolaev Institute of Inorganic Chemistry, Siberian Branch of Russian Academy of Sciences, 3, Akad. Lavrentiev Ave., Novosibirsk, 630090, Russia*

[b] *Novosibirsk State University (National Research University), Department of Natural Sciences, 2, Pirogova str., Novosibirsk, 630090, Russia*

[c] *N. N. Vorozhtsov Novosibirsk Institute of Organic Chemistry, Siberian Branch of Russian Academy of Sciences, 9, Akad. Lavrentiev Ave., Novosibirsk, 630090, Russia*

E-mail addresses: bushuev@niic.nsc.ru, mark.bushuev@gmail.com (M. B. Bushuev)

Table of contents

Table S1.

Crystal data and structure refinement for the compounds **1 – 3** and the ligands.

Compound	**1**	**2**	**3**	**L²**	**L³**
Empirical formula	$C_{92}H_{84}Br_6Cu_4N_{20}O_4$	$C_{46}H_{42}Cl_3Cu_2N_{10}O_2$	$C_{25}H_{18}Br_3Cu_2N_4O$	$C_{23}H_{21}N_5O$	$C_{25}H_{18}N_4O$
Formula weight	2267.41	1000.33	757.24	383.45	390.43
Crystal system	monoclinic	triclinic	monoclinic	monoclinic	orthorhombic
Space group	*C*2/*c*	$P\bar{1}$	$P2_1/n$	$P2_1/c$	*Pbca*
a(Å)	20.0008(5)	9.1159(2)	8.2845(2)	11.637(1)	7.9801(7)
b(Å)	18.3973(4)	13.6244(3)	12.2544(3)	7.5691(6)	18.569(2)
c(Å)	24.6565(7)	18.4950(4)	24.6190(7)	21.511(2)	26.854(3)
α(°)		74.008(1)			
β(°)	95.092(1)	85.516(1)	92.923	94.403(3)	
γ(°)		89.225(1)			
V(Å^3)	9036.8(4)	2201.32(8)	2496.11(11)	1889.2(3)	3979.1(7)
Z	4	2	4	4	8
T(K)	150(2)	150(2)	150(2)	150(2)	150(2)
D_{Calc}(g/cm^3)	1.667	1.509	2.015	1.348	1.303
μ (mm^{-1})	3.645	1.200	6.533	0.086 mm	0.082
Crystal size (mm^3)	0.45 x 0.11 x 0.10	0.42 x 0.35 x 0.21	0.25 x 0.22 x 0.18	0.25 x 0.21 x 0.15	0.45 x 0.05 x 0.05
Theta range for data collection (°)	1.66 - 26.37	1.66 - 26.37	1.66 - 26.37	1.76 – 26.37	2.19 – 26.02
Index ranges	-21≤ h ≤ 24	-11 ≤ h ≤ 11	-6 ≤ h ≤ 10	-14 ≤ h ≤ 14	-9 ≤ h ≤ 6
	-22 ≤ k ≤ 14	-10 ≤ k ≤ 17	-13 ≤ k ≤ 15	-9 ≤ k ≤ 5	-22 ≤ k ≤ 22
	-30 ≤ l ≤ 29	-22 ≤ l ≤ 23	-30 ≤ l ≤ 30	-26 ≤ l ≤ 26	-33 ≤ l ≤ 28
Reflections collected	27137	16421	16025	13728	22263
Independent reflections (R_{int})	9228 (0.0308)	8926 (0.0179)	5118 (0.0178)	3869 (0.0274)	3912 (0.0666)
Completeness to theta	100.0 % (25.50°)	99.1 % (25.50°)	100.0 % (25.50°)	99.9 (25.50°)	99.9 (25.50°)
Absorption correction	SADABS	SADABS	SADABS	SADABS	SADABS
Max. and min. Transmission	0.7119 and 0.2908	0.7867 and 0.6326	0.3859 and 0.2920	0.9872 and 0.9787	0.9959 and 0.9639
Refinement method	Full-matrix least-squares on F^2	Full-matrix least-squares on F^2	Full-matrix least-squares on F^2	Full-matrix least-squares on F^2	Full-matrix least-squares on F^2
Data / restraints / parameters	9228 / 0 / 570	8926 / 18 / 578	5118 / 0 / 316	3869 / 0 / 262	3912 / 0 / 272
Goodness-of-fit on F^2	1.050	1.055	1.039	1.043	1.008
Final *R* indices [*I*>2sigma(I)]	R_1 = 0.0314, wR_2 = 0.0693	R_1 = 0.0385, wR_2 = 0.0998	R_1 = 0.0195, wR_2 = 0.0432	R_1 = 0.0360, wR_2 = 0.0872	R_1 = 0.0403, wR_2 = 0.0862
R indices (all data)	R_1 = 0.0524, wR_2 = 0.0743	R_1 = 0.0383, wR_2 = 0.1037	R_1 = 0.0258, wR_2 = 0.0443	R_1 = 0.0510, wR_2 = 0.0919	R_1 = 0.0713, wR_2 = 0.0946
Largest diff. peak and hole (e/Å^3)	0.643 and -0.588	0.902 and -0.798	0.446 and -0.286	0.213 and -0.239	0.266 and -0.176

Table S2.

Selected bond lengths (Å) and angles [°] for the compounds **1** – **3**.

Compound **1**			
Bond	d	Angle	ω
Cu(1)-N(13)	1.962(2)	N(11)-Cu(1)-N(13)	79.32(8)
Cu(1)-N(23)	1.965(2)	N(11)-Cu(1)-N(23)	99.26(8)
Cu(1)-N(11)	2.084(2)	N(11)-Cu(1)-N(21)	102.71(8)
Cu(1)-N(21)	2.238(2)	N(13)-Cu(1)-N(23)	177.80(9)
Cu(1)-Br(1)	2.4386(4)	N(13)-Cu(1)-N(21)	105.34(8)
Cu(2)-Br(2)	2.3143(7)	N(11)-Cu(1)-Br(1)	156.53(6)
Cu(2)-Br(4)#1	2.4258(4)	N(13)-Cu(1)-Br(1)	92.40(6)
Cu(3)-Br(4)#1	2.4298(4)	N(21)-Cu(1)-N(23)	76.57(8)
Br(3)-Cu(3)	2.3192(6)	N(23)-Cu(1)-Br(1)	88.28(6)
Br(4)-Cu(2)	2.4258(4)	N(21)-Cu(1)-Br(1)	100.65(6)
Br(4)-Cu(3)	2.4298(4)	Br(2)-Cu(2)-Br(4)#1	125.08(1)
		Br(2)-Cu(2)-Br(4)	125.08(1)
Cu(2)-Cu(3)	2.7952(7)	Br(4)#1-Cu(2)-Br(4)	109.84(2)
		Br(3)-Cu(3)-Br(4)#1	125.21(1)
		Br(3)-Cu(3)-Br(4)	125.21(1)
		Br(4)#1-Cu(3)-Br(4)	109.57(2)
		Cu(2)-Br(4)-Cu(3)	70.29(2)
Compound **2**			
Bond	d	Angle	ω
Cu(1)-N(11)	2.236(3)	N(11)-Cu(1)-N(13)	76.29(10)
Cu(1)-N(13)	1.963(3)	N(11)-Cu(1)-N(21)	92.10(10)
Cu(1)-N(21)	2.153(3)	N(11)-Cu(1)-N(23)	96.71(10)
Cu(1)-N(23)	1.975(3)	N(11)-Cu(1)-Cl(11)	113.35(7)
Cu(1)-Cl(11)	2.2389(9)	N(13)-Cu(1)-N(21)	90.97(10)
Cu(2)-Cl(21)	2.055(10)	N(13)-Cu(1)-N(23)	166.64(11)
Cu(2)-Cl(22)	2.080(12)	N(13)-Cu(1)-Cl(11)	95.58(8)
Cu(3)-Cl(32)	2.088(3)	N(21)-Cu(1)-N(23)	77.78(10)
Cu(3)-Cl(31)	2.089(2)	N(21)-Cu(1)-Cl(11)	154.54(8)
		N(23)-Cu(1)-Cl(11)	97.66(8)
		Cl(21)-Cu(2)-Cl(22)	176.5(4)
		Cl(32)-Cu(3)-Cl(31)	178.32(9)
Compound **3**			
Bond	d	Angle	ω
Cu(1)-N(11)	1.9869(17)	N(11)-Cu(1)-N(13)	78.83(7)
Cu(1)-N(13)	1.9898(17)	N(11)-Cu(1)-Br(1)	103.28(5)
Cu(1)-Br(1)	2.3567(3)	N(13)-Cu(1)-Br(1)	133.65(5)
Cu(1)-Br(2)	2.3170(3)	N(11)-Cu(1)-Br(2)	140.42(5)
Cu(2)-N(14)	2.0835(16)	N(13)-Cu(1)-Br(2)	101.64(5)
Cu(2)-Br(3)	2.4584(3)	Br(2)-Cu(1)-Br(1)	104.07(1)
Cu(2)-Br(1)#1	2.4516(3)	N(14)-Cu(2)-Br(1)#1	112.17(5)
Cu(2)-Br(3)#2	2.5402(3)	N(14)-Cu(2)-Br(3)	106.42(5)
		Br(1)#1-Cu(2)-Br(3)	111.81(1)
Cu(2)-Cu(2)#2	2.9199(5)	N(14)-Cu(2)-Br(3)#2	100.45(5)
		Br(1)#1-Cu(2)-Br(3)#2	116.48(1)
		Br(3)-Cu(2)-Br(3)#2	108.54(1)

Symmetry transformations used to generate equivalent atoms: for **1**: #1 -x,y,-z+1/2; for **3**: #1 -x+1,-y+1,-z #2 -x+2,-y+1,-z

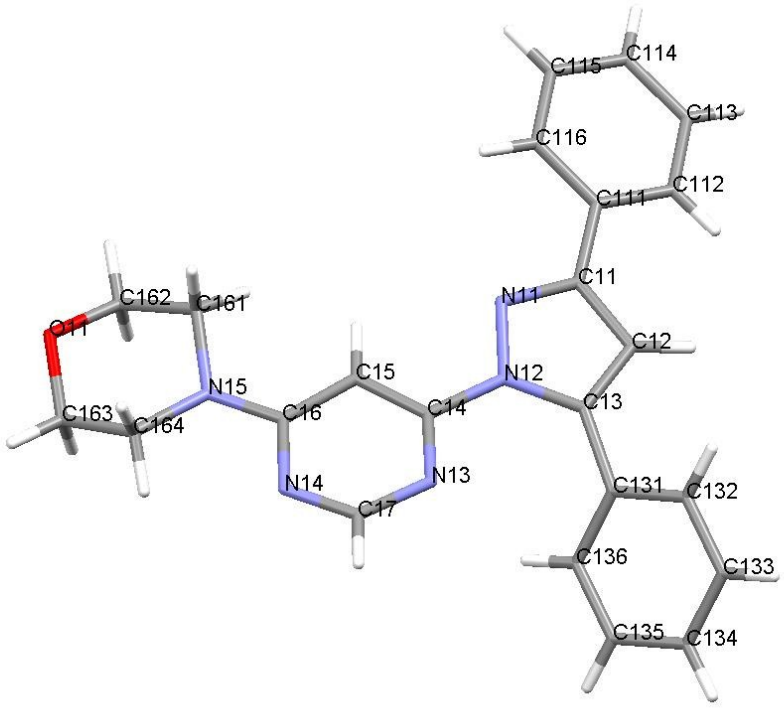

Figure S1. Molecular structure of **L¹**.

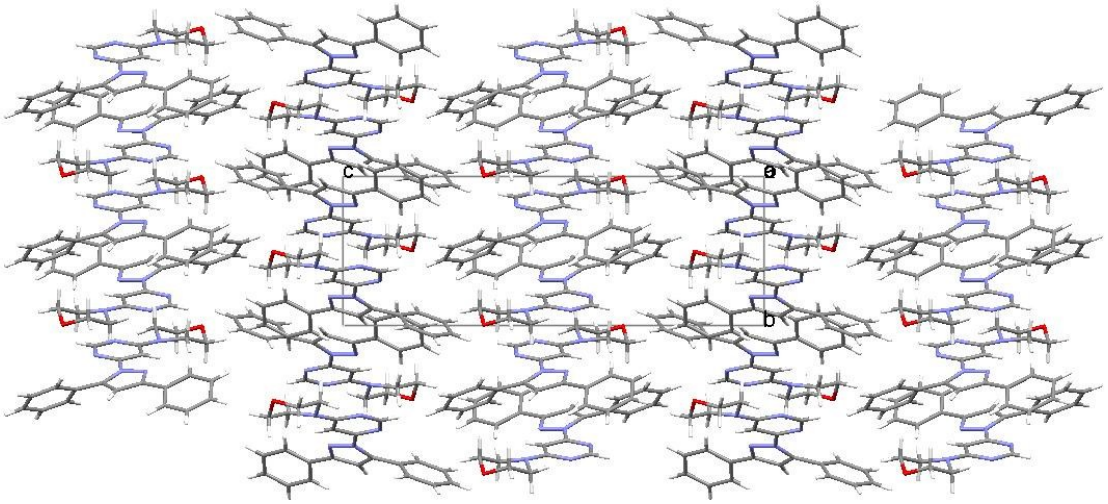

Figure S2. Packing diagram for **L²** (view along the *a*-axis).

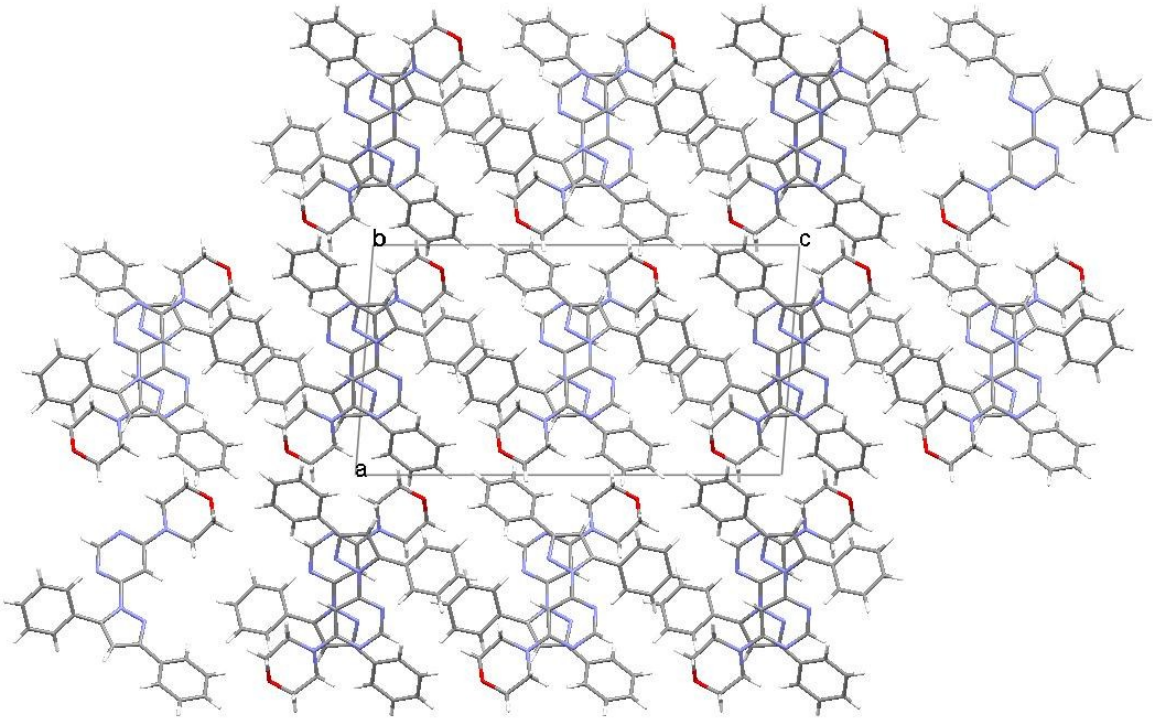

Figure S3. Packing diagram for **L²** (view along the *b*-axis).

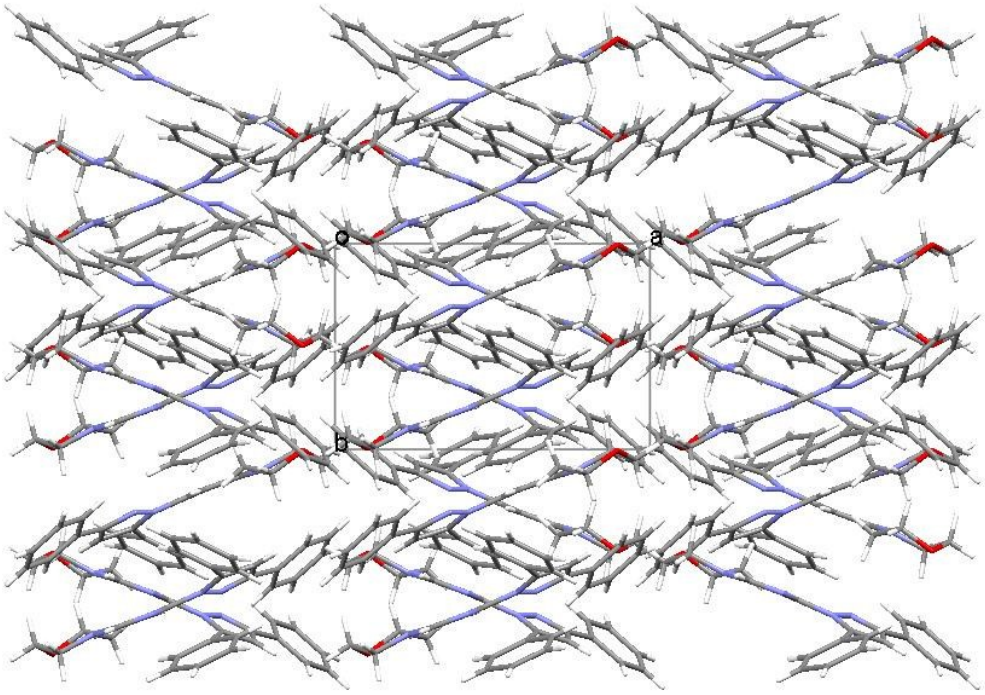

Figure S4. Packing diagram for **L²** (view along the *c*-axis).

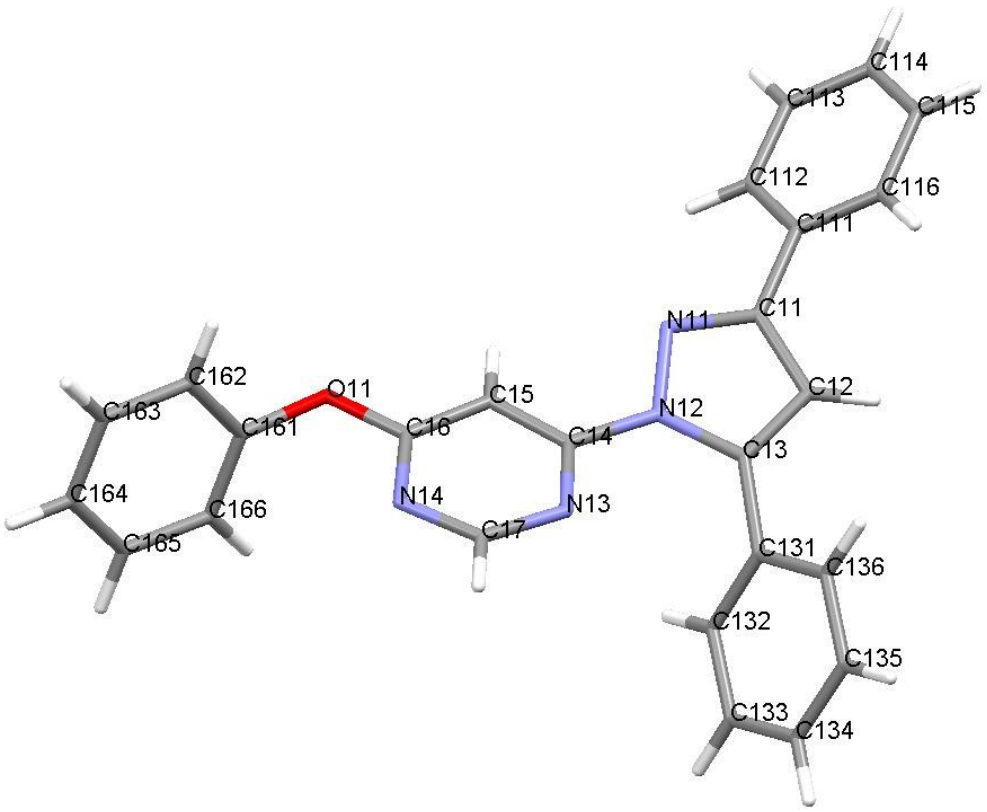

Figure S5. Molecular structure of **L³**.

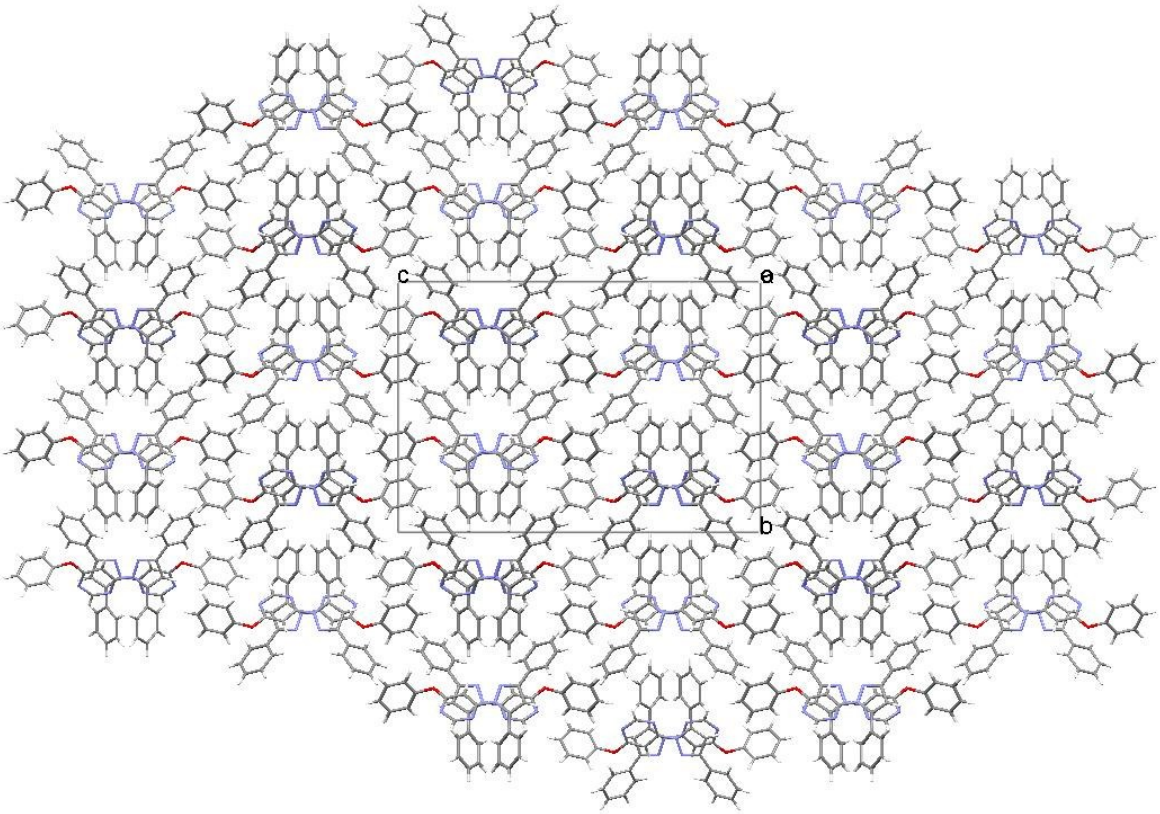

Figure S6. Packing diagram for **L³** (view along the *a*-axis).

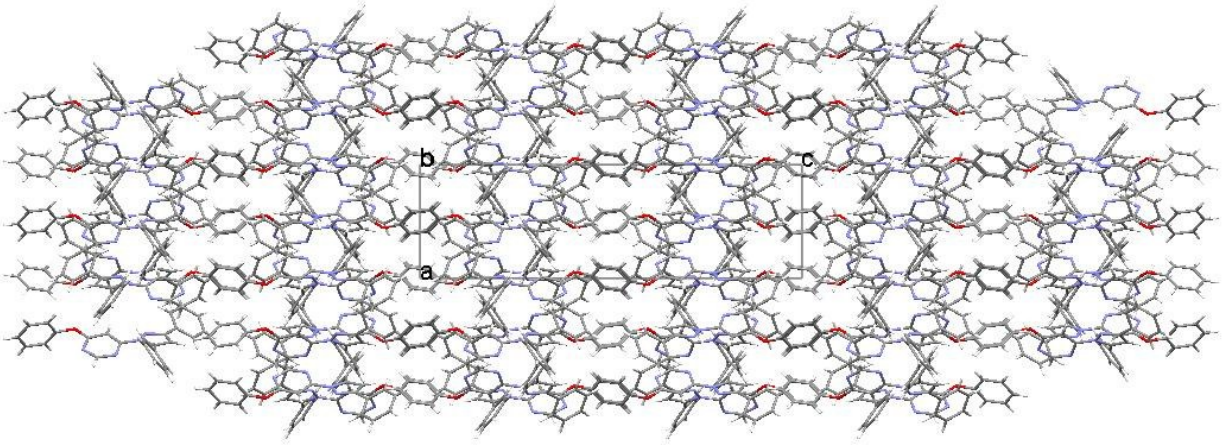

Figure S7. Packing diagram for **L³** (view along the *b*-axis).

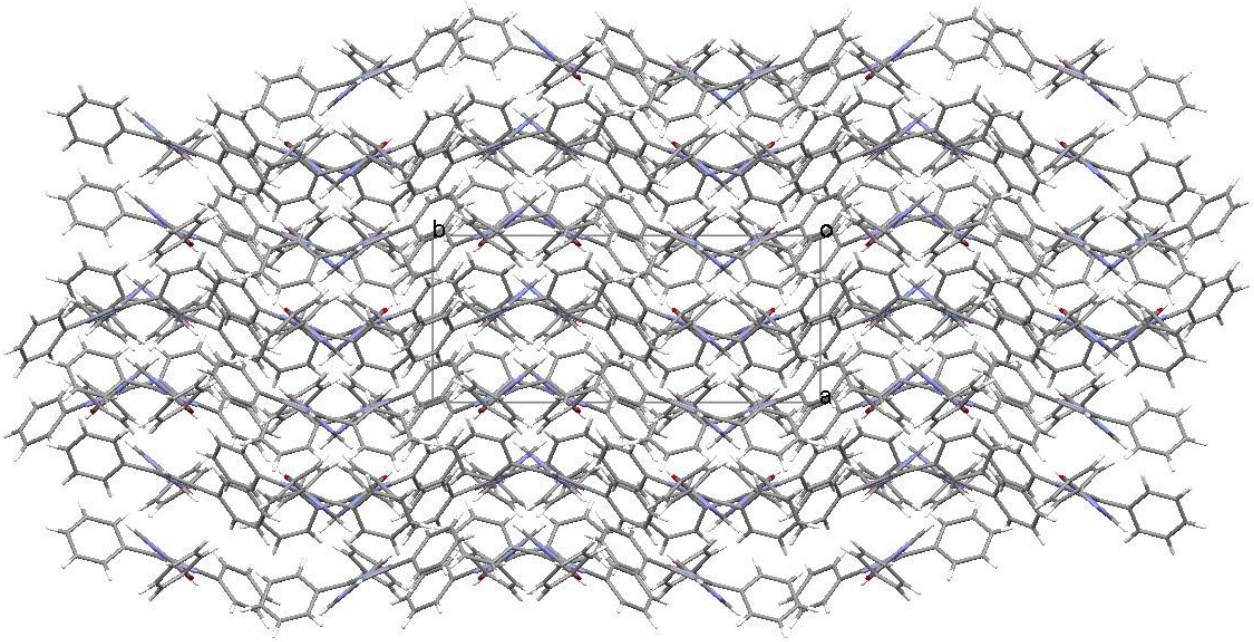

Figure S8. Packing diagram for **L³** (view along the *c*-axis).

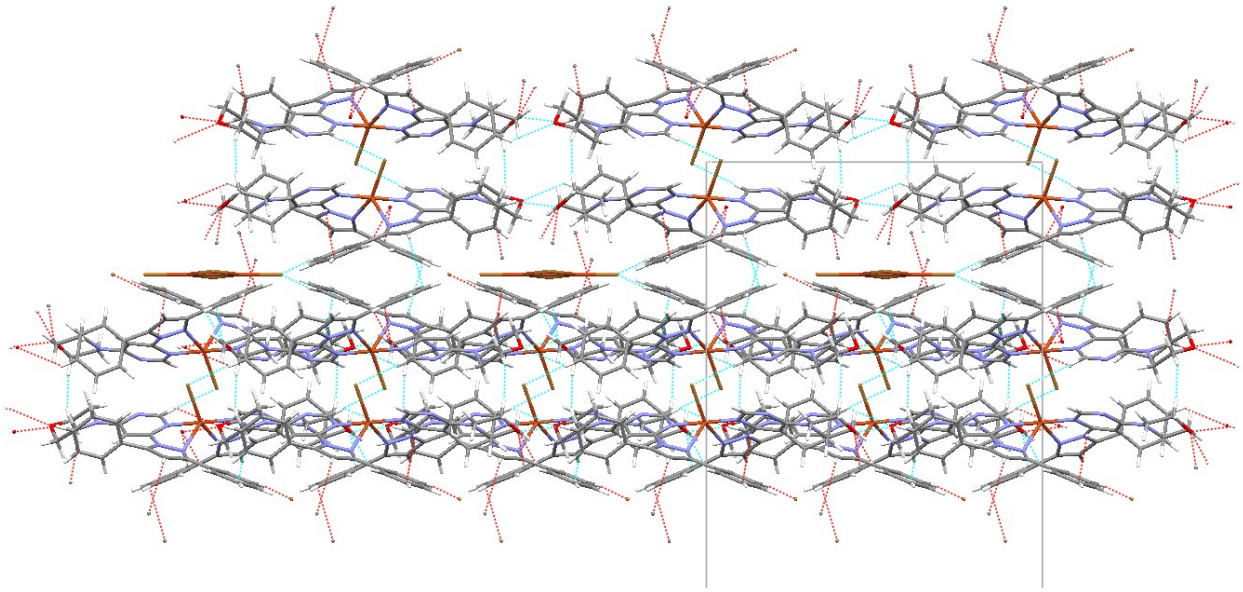

Figure S9. Packing of 1D double chains in the structure of **1**. View along the *a*-axis, three double chains are shown (side view).

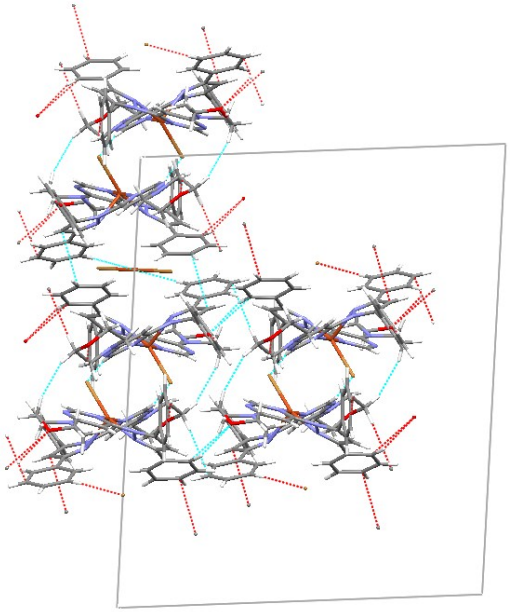

Figure S10. Packing of 1D double chains in the structure of **1**. View along the *b*-axis, three double chains are shown (view along the chains).

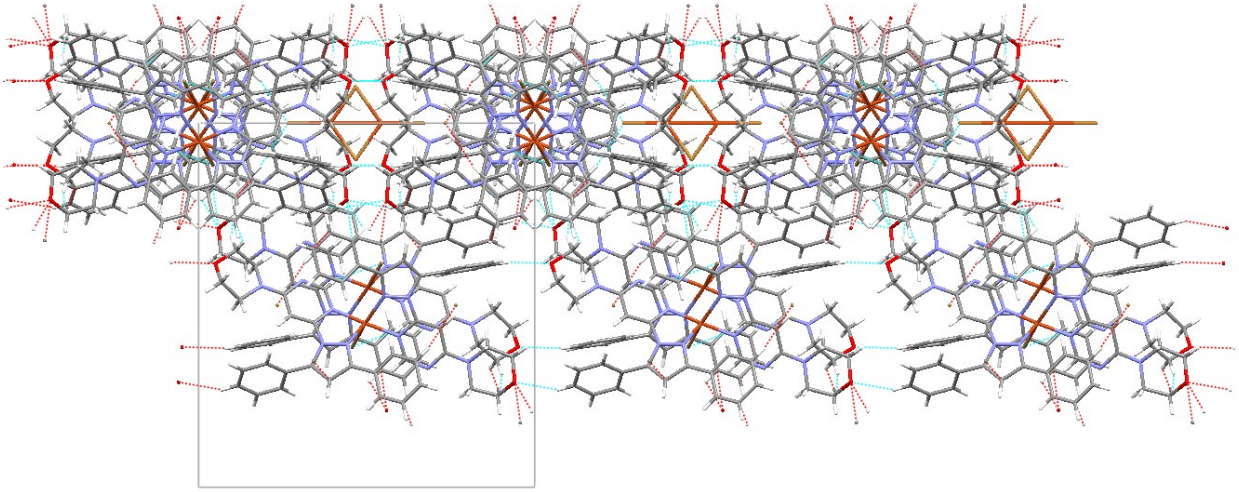

Figure S11. Packing of 1D double chains in the structure of **1**. View along the *c*-axis, three double chains are shown (side view).

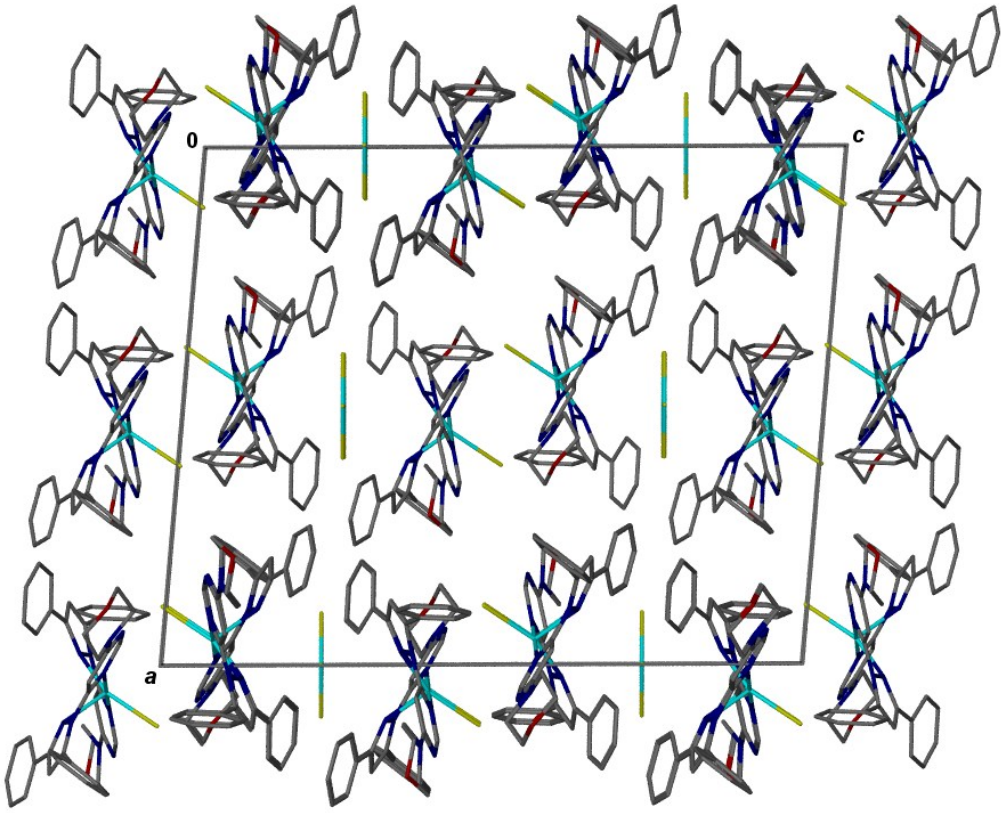

Figure S12. Supramolecular structure of **1**. View along the *b*-axis.

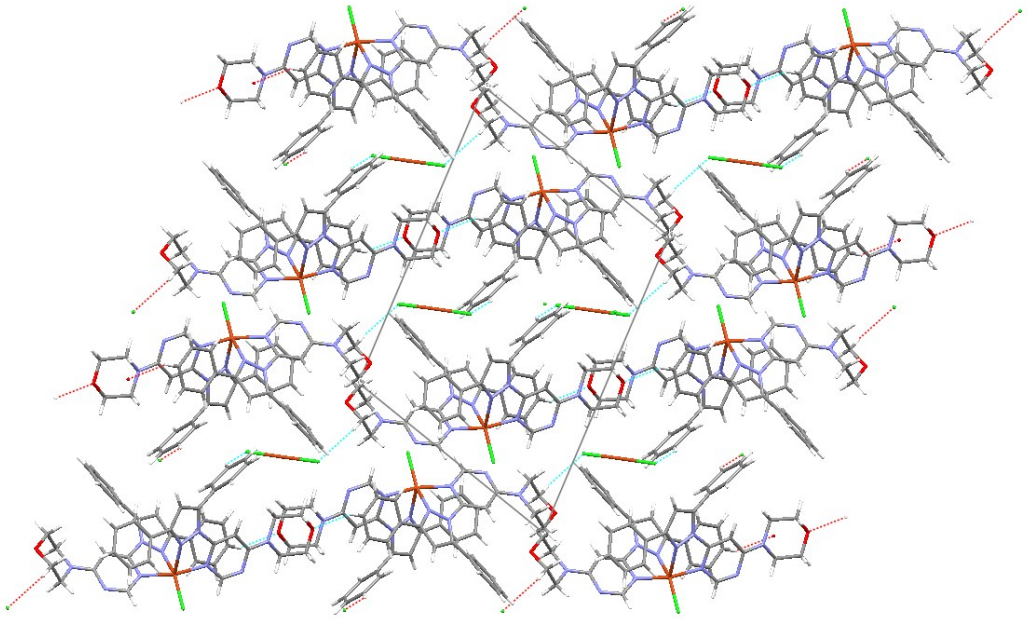

Figure S13. 2D layer in the structure of **2**. View along the *a*-axis.

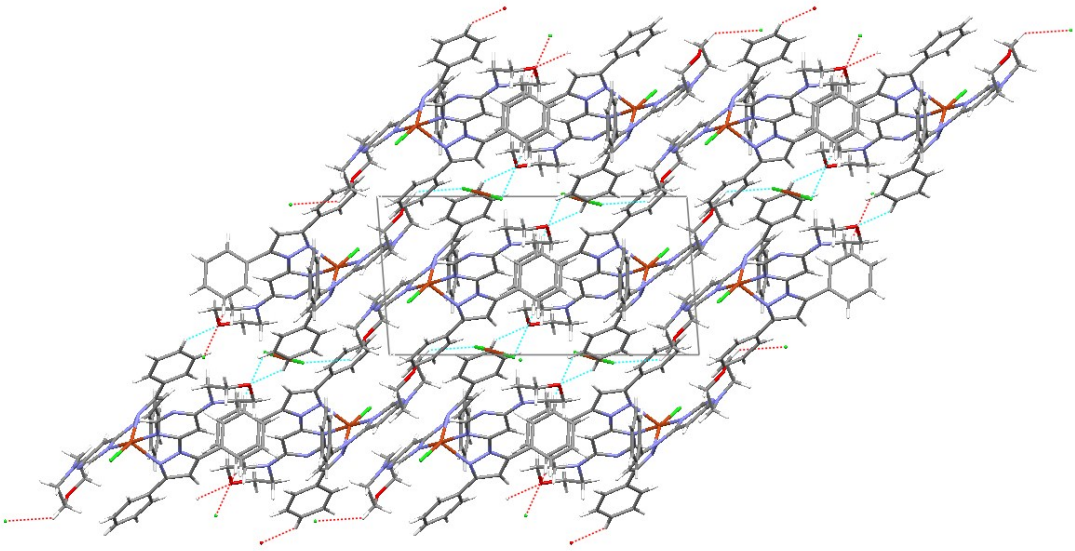

Figure S14. 2D layer in the structure of **2**. View along the *b*-axis.

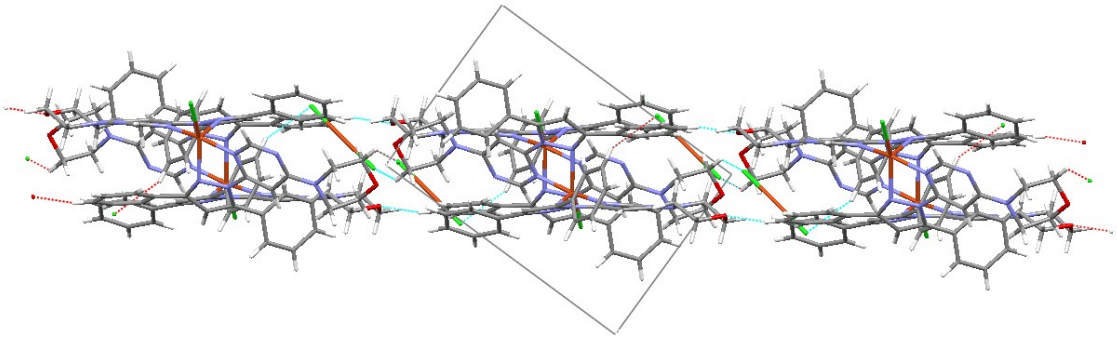

Figure S15. 2D layer in the structure of **2**. View along the *c*-axis (side view).

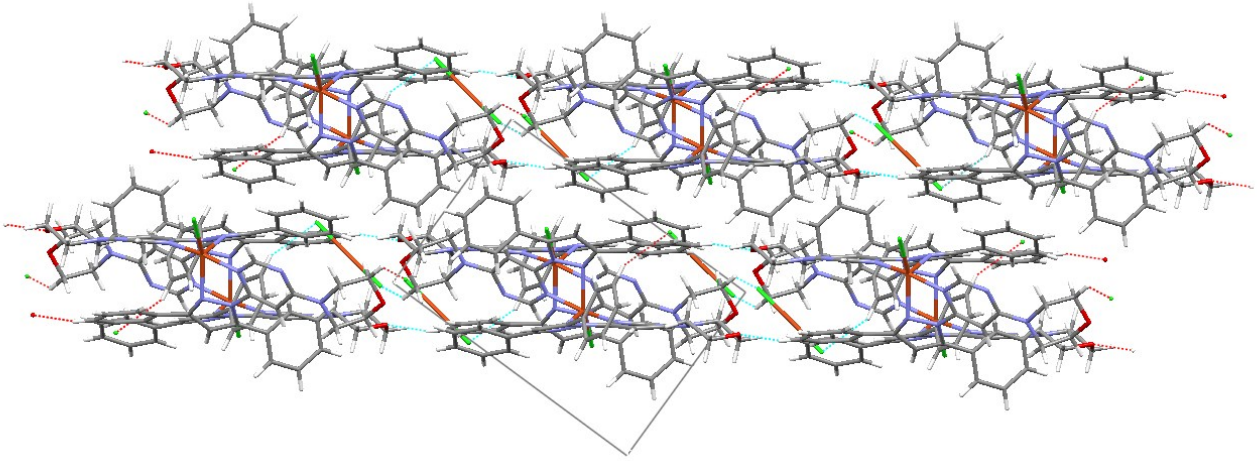

Figure S16. Packing of 2D layers in the structure of **2**. View along the *c*-axis (side view, two layers are shown).

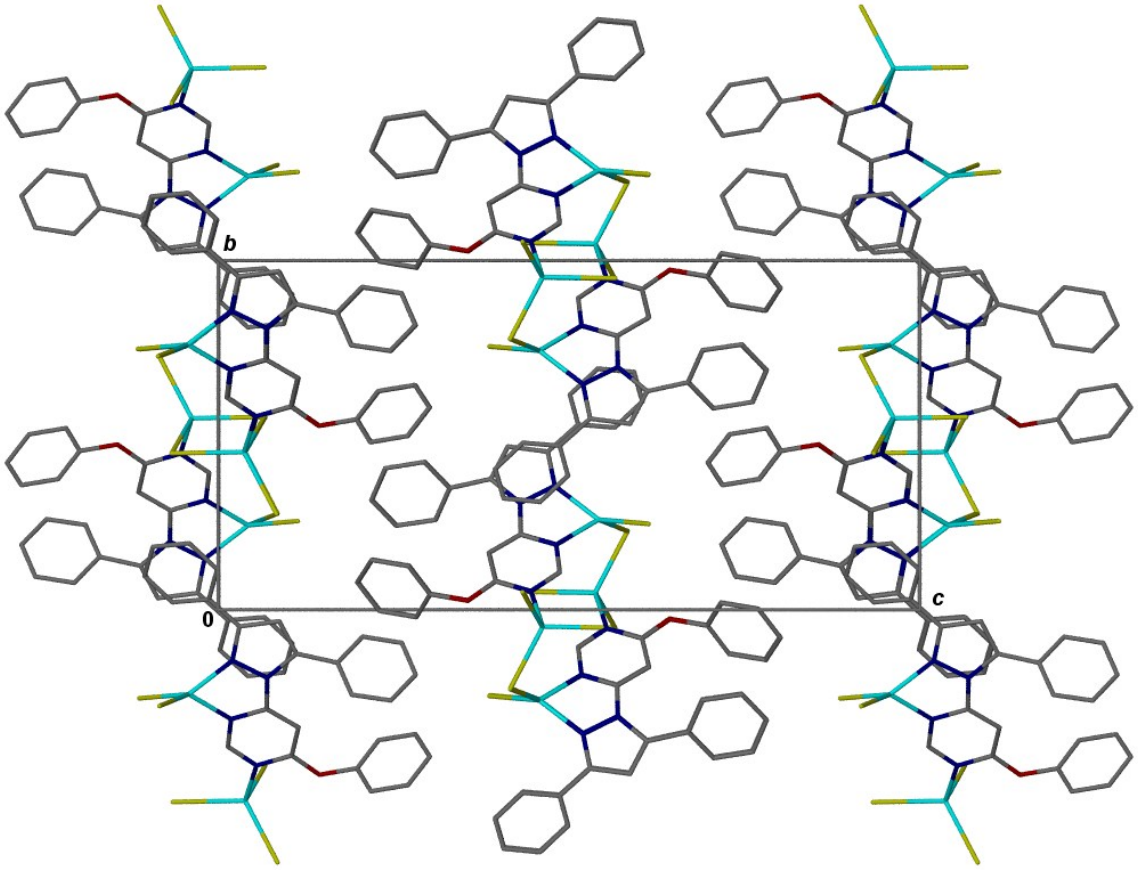

Figure S17. Packing of 2D layers in the structure of **3**. View along the *a*-axis (three layers are shown, hydrogen atoms are omitted for clarity).

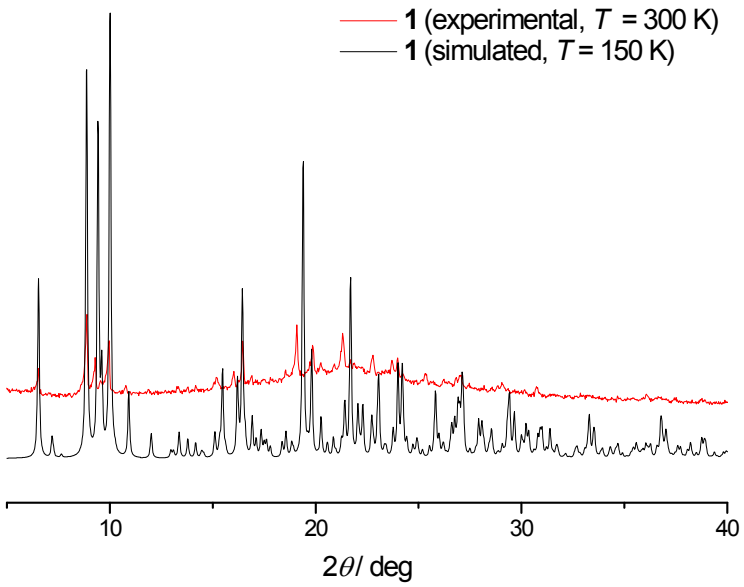

Figure S18. Experimental and simulated X-ray powder patterns for the complex **1**.

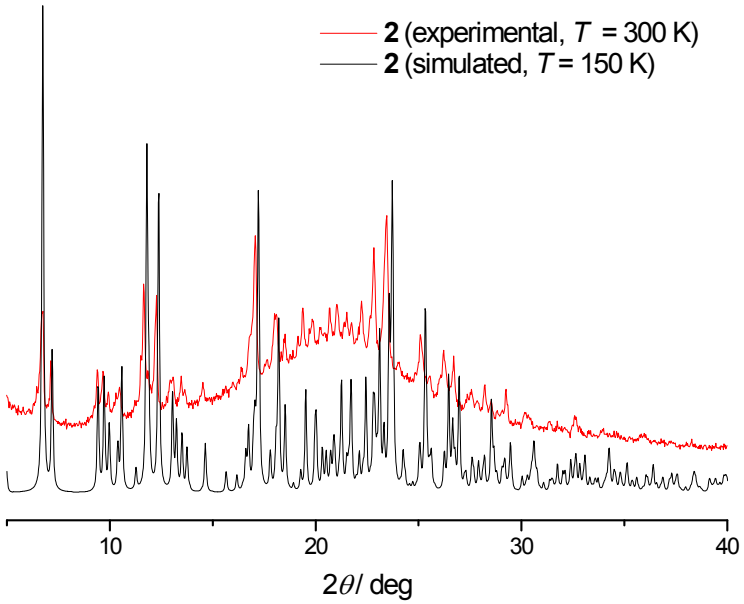

Figure S19. Experimental and simulated X-ray powder patterns for the complex **2**.

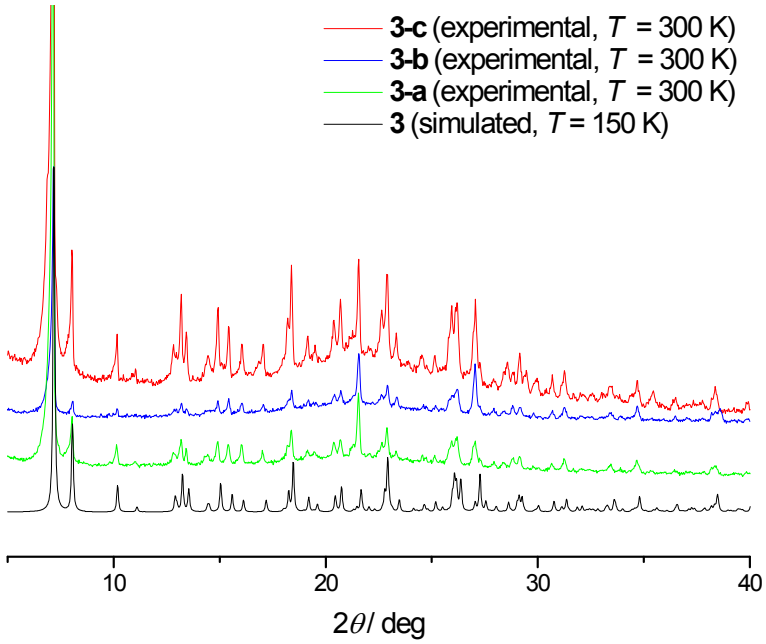

Figure S20. Experimental and simulated X-ray powder patterns for the complex **3**.

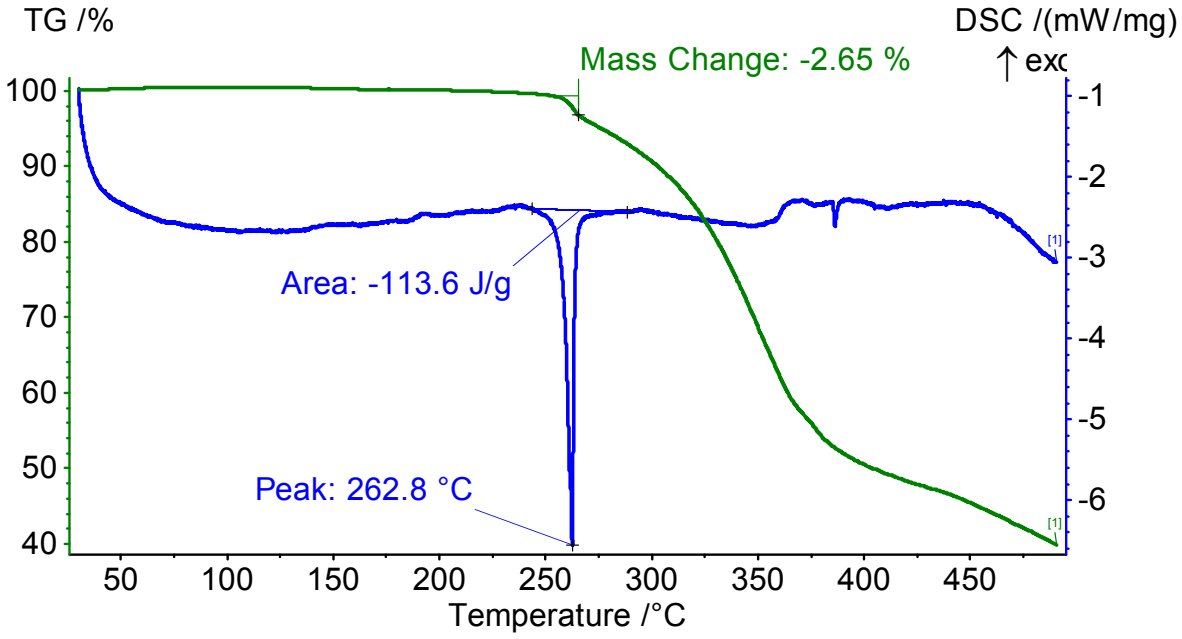

Figure S21. TGA and DSC curves for the complex **3-a**.

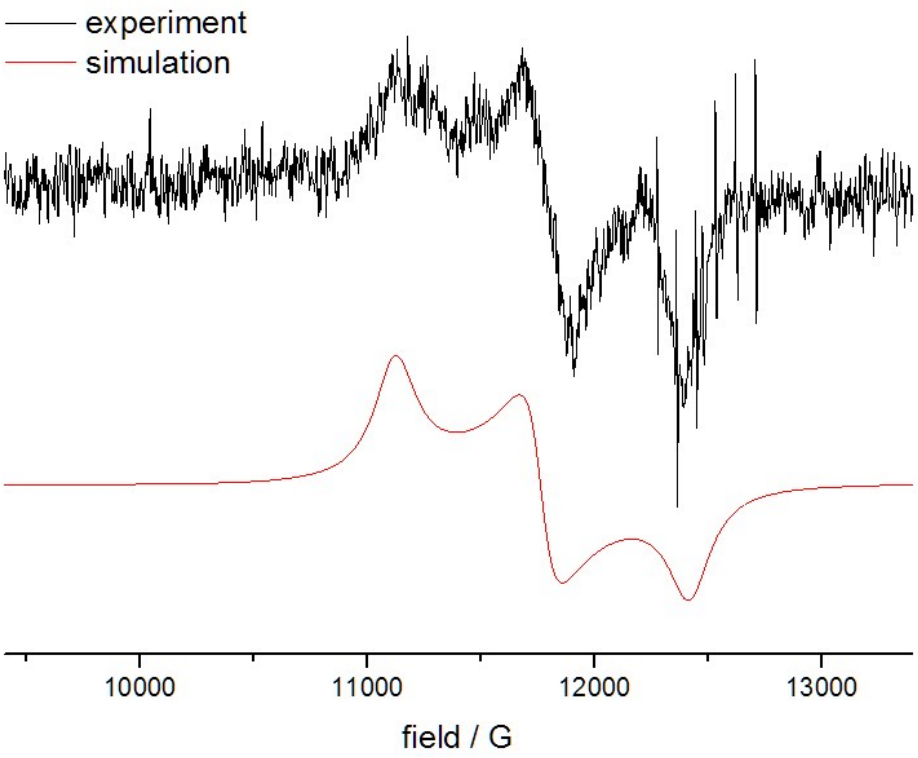

Figure S22. EPR spectrum for the complex **2**.

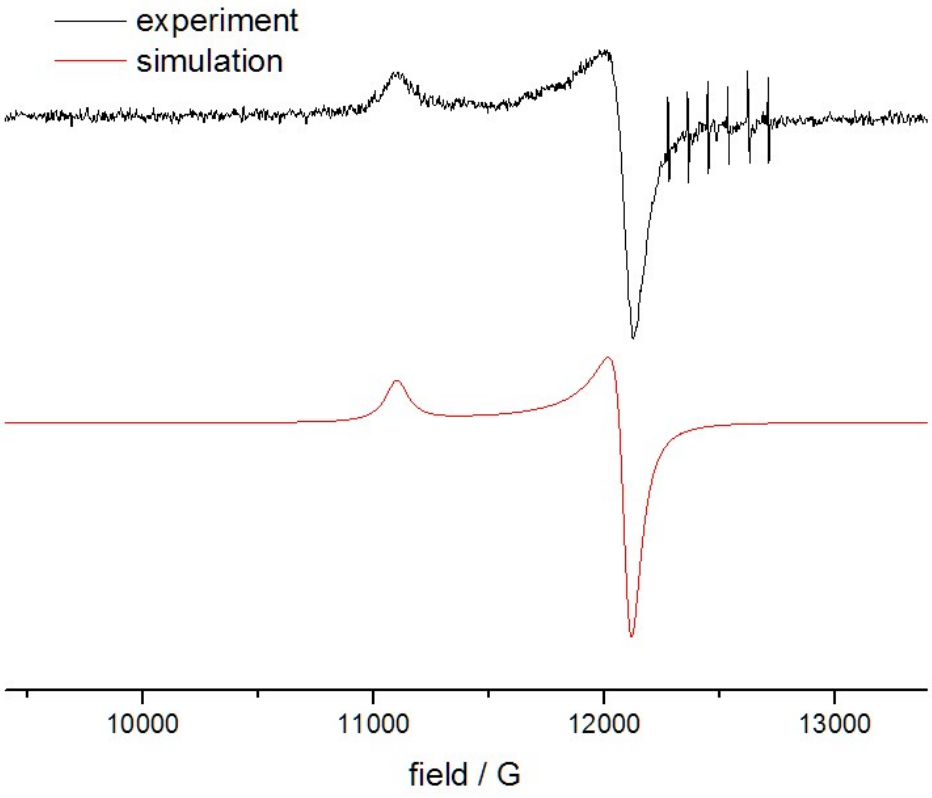

Figure S23. EPR spectrum for the complex **3**.